SAND97-0601C
SAND--97-0601C [1]
CONF-970232--6

Criteria determining the selection of slags for the melt decontamination of radioactively contaminated stainless steel by electroslag remelting

Joanna M.R. Buckentin[a], David G. Atteridge[b], Brian K. Damkroger[a], and Gregory J. Shelmidine[a]

[a]Sandia National Laboratories
Albuquerque, NM

[b]Oregon Graduate Institute of Science & Technology
Beaverton, OR

MASTER

ABSTRACT

Electroslag remelting is an excellent process choice for the melt decontamination of radioactively contaminated metals. ESR furnaces are easily enclosed and do not make use of refractories which could complicate thermochemical interactions between molten metal and slag. A variety of cleaning mechanisms are active during melting; radionuclides may be partitioned to the slag by means of thermochemical reaction, electrochemical reaction, or mechanical entrapment. At the completion of melting, the slag is removed from the furnace in solid form. The electroslag process as a whole is greatly affected by the chemical and physical properties of the slag used. When used as a melt decontamination scheme, the ESR process may be optimized by selection of the slag. In this research, stainless steel bars were coated with non-radioactive surrogate elements in order to simulate surface contamination. These bars were electroslag remelted using slags of various chemistries. The slags investigated were ternary mixtures of calcium fluoride, calcium oxide, and alumina. The final chemistries of the stainless steel ingots were compared with those predicted by the use of a Free Energy Minimization Modeling technique. Modeling also provided insight into the chemical mechanisms by which certain elements are captured by a slag. Slag selection was also shown to have an impact on the electrical efficiency of the process as well as the surface quality of the ingots produced.

DISTRIBUTION OF THIS DOCUMENT IS UNLIMITED

DISCLAIMER

Portions of this document may be illegible in electronic image products. Images are produced from the best available original document.

INTRODUCTION

The downsizing or discontinuation of domestic nuclear operations, both defense related and commercial, has led to a growing stockpile of radioactively contaminated scrap metal, much of which is stainless steel. Due to initial design requirements for nuclear operations, this steel, which contains large quantities of strategic elements such as nickel and chromium, is the product of complex processing operations and thus represents a valuable domestic resource. A significant portion of the radionuclides of concern are present in the form of surface contamination.[1] An example is the oxidized material which is known to adhere tenaciously to the internal surfaces of reactor piping. This material is composed of corrosion products from anything with which the water has come in contact, including activated structures in the vicinity of the reactor core or fuel fragments which have escaped through cladding breaches.

Burial of contaminated metals would be wasteful and expensive, since long term monitoring would be necessary in order to minimize environmental risk. Surface decontamination methods are inexpensive, uncomplicated, and relatively effective for the removal of surface contamination from parts with simple geometries. However, these techniques are ineffective for removal of contamination from cracks, a common flaw in reactor steam and heat exchanger tubes. Melt decontamination processes allow the metal to be consolidated while radionuclides are partitioned to a gas or slag phase.

This paper addresses the melt decontamination of radioactively contaminated stainless steel by Electroslag Remelting. Electroslag Remelting, often referred to as ESR, is a secondary melting technique which may be used for a variety of metals and alloys. The ESR process is widely used among producers of specialty metals and alloys because it is capable of producing very clean material with an absence of pipe and porosity. Material produced by ESR has uniform structure and chemical composition and thus exhibits excellent mechanical properties. Optimized control strategies and correct slag selection result in smooth ingot surfaces, eliminating the need for surface treatment before working. Electroslag remelting is an excellent process choice for the melt decontamination of radioactively contaminated materials. ESR furnaces are easily enclosed to facilitate the capture of volatiles. The ESR process does not make use of refractories, which could complicate thermochemical reactions between molten metal and slag and could be a source of cross-contamination between melts. When used as a melt decontamination strategy, ESR maintains the specified chemistry and mechanical properties of the original material while capturing the radioactive transuranic elements in a stable slag phase. Radioactive metal decontaminated in this fashion is suitable for direct fabrication and controlled reuse within the nuclear community.

MELTING AND MODELING STUDIES

The specific purpose of this study was to determine the effects of slag chemistry on the melt decontamination efficiency achieved by ESR when 304L stainless steel was melted in contact with various slags having different ratios of $CaF_2/CaO/Al_2O_3$. Selected non-radioactive rare earth elements were used in these experiments to simulate the presence of radioactive transuranic elements. Thermodynamic modeling was performed in order to predict the differences which could be expected in the behaviors of the surrogate elements and actual radionuclides in a high temperature environment.

Choice of Surrogates

Due to complications involved with work involving radioactive materials, surrogate elements were chosen which mimic, as accurately as possible, the chemical and thermodynamic behaviors of the radionuclides of interest. The radionuclides of interest in this work are fission products which include rare earth elements, cesium, strontium and actinide elements, primarily uranium, thorium, plutonium, and americium. These nuclides are largely by products of uranium beneficiation, enrichment, reactor fuel reprocessing, and weapons program activities.

One means of comparing the thermochemical similarities of elements is by the comparison of the stabilities of their oxides by means of an Ellingham diagram. Figure 1 shows the free energy of formation of various stable oxides, normalized per mole of oxygen.

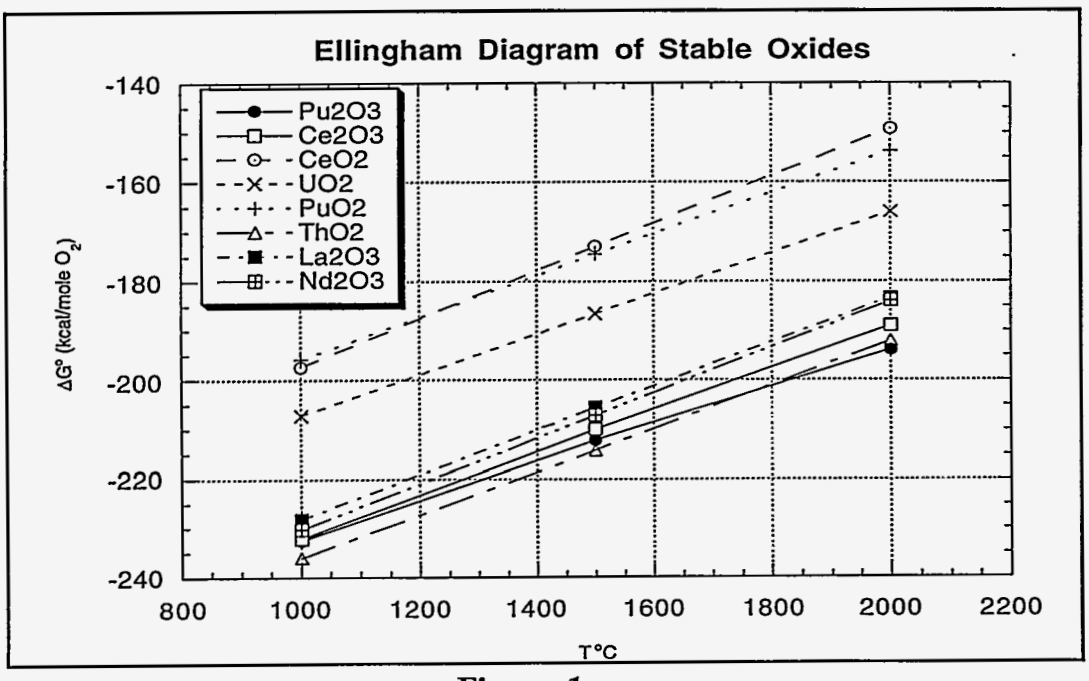

Figure 1
Comparison of the Stabilities of Oxides of Radionuclides and Surrogates

Figure 1 may be used to determine how closely the surrogates are likely to mimic the radionuclides in their tendency to form stable oxides. If, for example, plutonium exists in its +4 oxidation state, it is well represented by cerium in its +4 oxidation state. If plutonium is present in its +3 oxidation state it may be represented by either cerium in its +3 state, or by lanthanum or neodymium. The free energy of ThO_2 is comparable to those of La_2O_3 and Nd_2O_3, but its oxidation state is different. Uranium is best represented by cerium in its +4 oxidation state.

Melt Stock Preparation

Bars of 304L stainless steel measuring 2' long by 2.5" in diameter were coated with oxides of cerium and lanthanum to mimic the presence of oxidized surface contamination. In order to insure production of a tenacious, non-friable, coating surrogate oxide powders were co-sprayed along with a stainless steel wire addition. The elemental concentrations for each stainless steel bar were approximately 1000 ppm of cerium and 1000 ppm of lanthanum.

Selection and Preparation of Slags

The most widely used slag systems in ESR are those in the calcium fluoride-lime-alumina system. The chemistry of ESR slag influences such important physical properties as resistivity and heat capacity, as well as density, viscosity, and surface tension. Resistivity influences the efficiency of the ESR process, as the heat necessary for melting is generated by the resistive heating of the slag. Viscosity affects the residence time of metal droplets in the slag, the rate of escape of gasses, the degree of stirring in the slag, the kinetics of mass transfer, and the thickness of the slag skin.[2,3] The difference in density between the slag and the metal also has an effect on the residence time and size of droplets. The interfacial tension between slag and metal should have a low value to increase mass transfer rate and facilitate the production of small droplets, but this can reduce the ability of slag and metal to separate and thus encourage slag entrapment. Surface tension also affects the mechanism of solution of inclusions as well as the surface quality of the ingot produced.

Salt[4] suggested a notation to describe slag composition. Calcium fluoride is listed first followed by the remaining constituents in the order of lime, magnesia, alumina, and silica (which is the order of decreasing basicity) giving their percentage compositions only. The general formula is (a/b/c/d/e) where a=% calcium fluoride, b=% lime, c= % magnesia, d=% alumina, and e=% silica. Slag compositions within the ternary calcium fluoride-lime-alumina system are abbreviated by the shorthand of writing (%CaF_2/% CaO/% Al_2O_3).

The slags investigated in this work were made up of ternary mixtures of calcium fluoride, calcium oxide, and alumina as shown in Figure 2. Slags were blended from their constituent oxides and prefused in a graphite crucible.

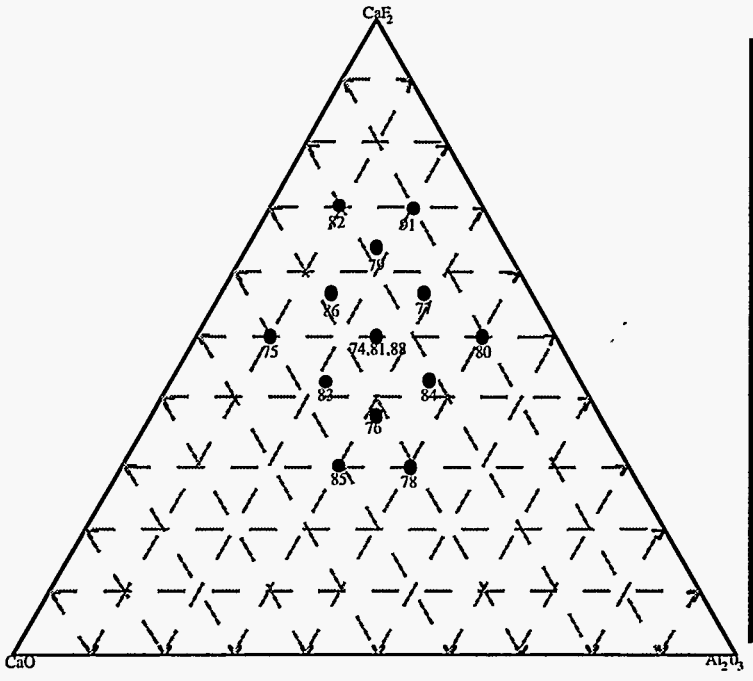

Slag Used $CaF_2/CaO/Al_2O_3$	Heat Number
50/25/25	89
50/25/25	93
50/25/25	90
50/25/25	74
50/40/10	75
36.6/31.7/31.7	76
56.7/15/28.3	77
30/30/40	78
63.4/18.3/18.3	79
50/10/40	80
50/25/25	81
70/20/10	82
43.3/35/21.7	83
43.3/21.7/35	84
30/40/30	85
56.7/28.3/15	86
70/10/20	91
50/25/25	88
50/25/25	92
50/25/25	94

Figure 2
Chemistries of Slags Plotted on Ternary Grid

Melting Experiments

Each surrogate coated stainless steel bar was melted into a 4" round mold. The slag charge for each melt was 1800 grams. The melt rate was held constant at 0.4 kg/min in order to keep the amount of molten steel in contact with the molten slag constant throughout the melt. At the completion of each melt, the slag skin and the slag cap were collected separately and weighed. Skin thicknesses were measured and the slag was examined for the presence of interesting structures. Representative samples were split and analyzed by Inductively Coupled Plasma Mass Spectrometry (ICP-MS). From each ingot produced, a slice was cut from a location where steady state melting had been achieved and electrode heating had not yet begun. Each slice was drilled from the outer radius in. Drill turnings from the first quarter inch of drill travel were collected for surface chemistry. Drill turnings for the subsequent one half inch of travel were collected for bulk chemistry. One quarter of the ingot slice was submitted for spectrographic analysis of the major elements.

Thermodynamic Modeling

The thermodynamic principle which makes melt refining possible is the fact that an element will partition between a metal and a slag toward an equilibrium in which its activity is the same in both phases.[5] In order to model a complex system, such as the interaction between molten stainless steel and a multicomponent slag, appropriate solution models must be use so that free energy minimization techniques may be employed. Free energy minimization was performed by use of software developed by the Facility for the Analysis of

Chemical Thermodynamics[6] (F*A*C*T*). The code calculates the equilibria of chemical systems by considering condensed species of invariant composition and solutions of species which could be present under equilibrium conditions. These solutions may be specified by the user to behave ideally or to conform to a given solution model.

Metallic species, present as liquids at the temperatures given, were grouped to form a liquid solution and were assigned to behave according to a modified dilute interaction parameter model developed by Pelton and Bale[7]. Oxygen and fluorine bearing species, which were liquid at the temperatures given, were allowed to form a slag phase which was assumed to behave as an ideal solution. Components of the system which were predicted to be solids at the temperature given were taken to be condensed phases of invariant composition. So that comparisons could be made between melting and modeling data, each melting experiment was modeled by free energy minimization techniques. Simulations were performed at an assumed melting temperature of 1700°C and one atmosphere of pressure.

RESULTS AND DISCUSSION

Ingot Chemistry

Each stainless steel ingot produced was analyzed in order to determine how melting in contact with various slags had changed the chemistry of the alloy. The chemistry changes associated with remelting stainless steel are important in terms of producing an alloy which meets the chemical specifications of the final product to be produced. In the case of nonsensitizing stainless steels, a maximum allowable limit is specified for carbon. Stainless steels which meet the chemical specifications for a particular grade and also have carbon levels lower than the maximum specified amount carry an L designation, such as 304L and 316L. In most cases, remelting did not cause the steel to deviate from the chemistry for 304L. All slags were found to remove manganese, silicon, and sulfur from the steel. Desulfurization was expected due to the known tendency for the rare earth elements to form stable oxysulfides of the form $(RE)_2O_2S$.[8,9,10].

Thermodynamic modeling was performed to quantitatively predict the transfer of elements from the liquid steel into the slag phase and to determine the compounds which may be formed by these elements in the slag phase. The distribution of an element between a metal and a slag is related to the amount of any species formed by the element when it contacts the slag phase. Modeling results showed that the amount of any species is governed not only by its own stability, but by the stability of other compounds with which it may compete for the elements of which it is composed.

For example, the predicted loss of manganese predicted by the model was compared with that observed in the melting experiments. For some heats, the model accurately predicted the manganese removal from steel, while for others, the loss was overestimated. The greatest discrepancy between melting and modeling occurs for heats in which slags low

in calcia were used. Figure 3 shows the effect of the calcia content of the slag on the predicted and actual manganese losses.

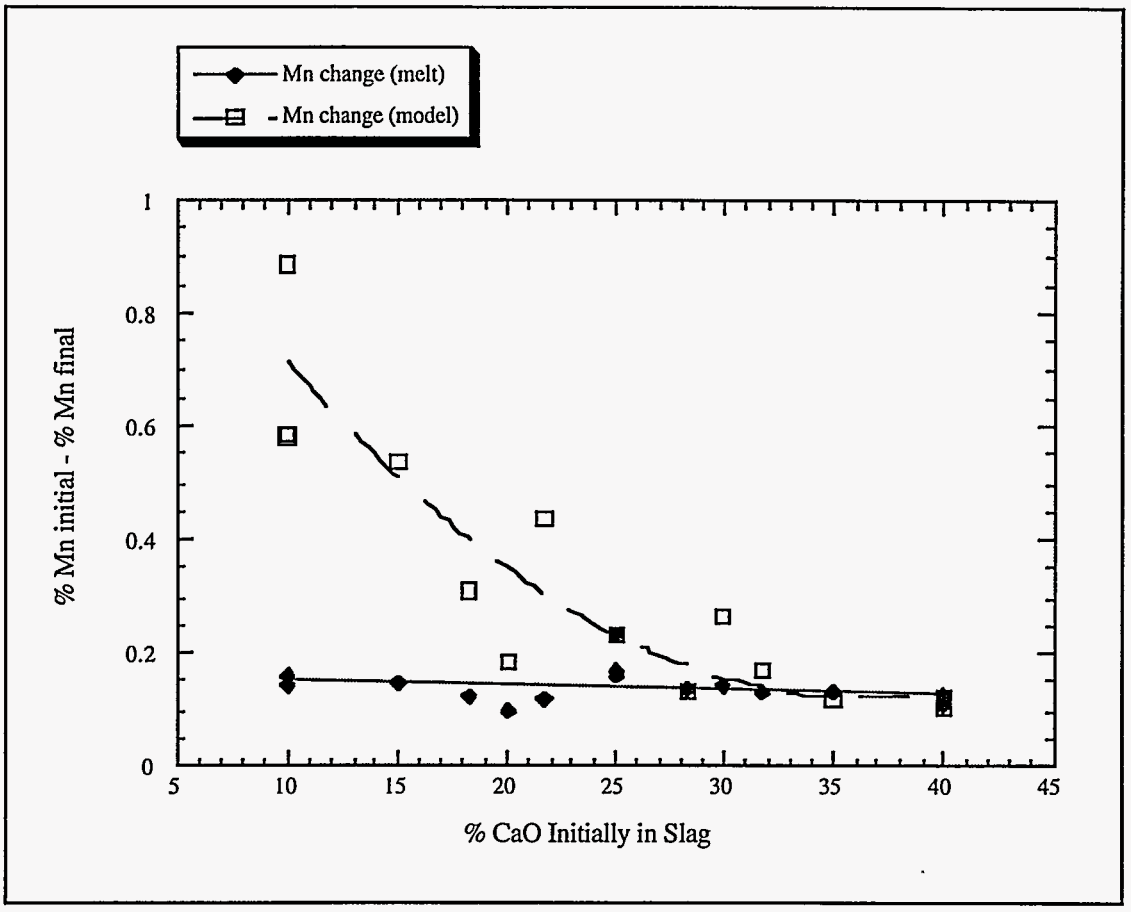

Figure 3
Comparison of Predicted and Actual Manganese Loss

For the heats which showed the most deviation the model had predicted the formation of increased quantities of $MnAl_2O_4$. The results indicate that this compound may not form to the extent predicted when an ideal solution model is used for the slag, as was done in this case. Further work is necessary to develop and benchmark a solution model for ESR slags which allows more accurate predictions to be made.

Removal of Surrogate Elements

Each ingot was analyzed for the presence of surrogate elements, both on the surface and in the bulk metal. Melting results showed that the surrogate elements were removed to below the detectable limit (1 ppm) regardless of the slag used except when slag was entrained on the surface of the ingot. Surrogate levels of 3-5 ppm were found in samples taken from the surfaces of two ingots with very poor surface quality, indicating that when slag choice results in poor surface quality, incomplete decontamination may be achieved. Free energy minimization studies predicted that surrogate levels would be much less than 1 ppm in the remelted steels, but that some slags would achieve more effective decontamination than others. For each slag/metal interaction modeled, free energy minimization predicted that

residual cerium concentrations would be less than 0.02 ppm and residual lanthanum concentrations would be below 0.0002 ppm for melts conducted at 1700°C. Although modeling predicted that the steel would be decontaminated to below the detectable limits, testwork was performed to determine whether or not the predicted decontamination would actually occur.

Modeling predicted that some slags would remove contaminants from steel more effectively than others, depending on the compounds formed by the contaminant in the slag, the availability of the elements needed in order for the compounds to form, and the thermodynamic driving force governing their formation. Lanthanum was predicted to be more effectively removed from the steel than cerium, as its fluoride and oxysulfide compounds are slightly more stable than those formed by cerium. The ability of a slag to effect the removal of an element from a steel hinges upon the types and quantities of compounds which may be formed by the element and available ions in the slag. Cerium and lanthanum may be removed from the steel by the formation of stable oxides, fluorides, oxysulfides, and oxyaluminates. In order to determine which slags are predicted to best remove surrogate elements from the metal, the residual cerium in the steel was compared on a heat by heat basis in Figure 4.

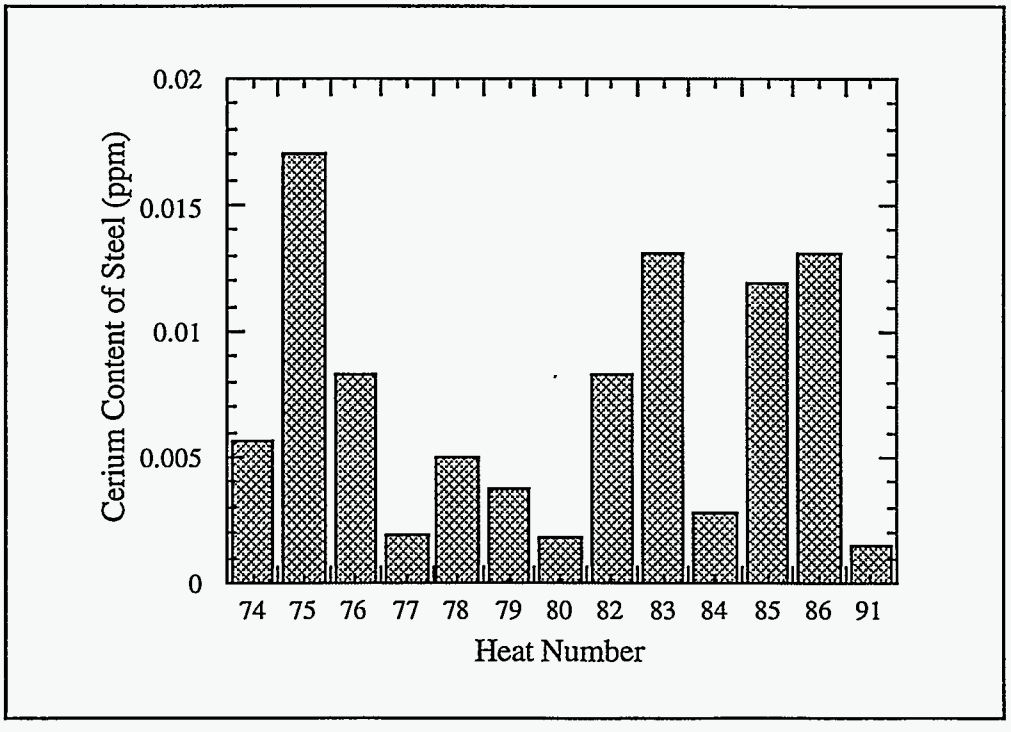

Figure 4
Predicted Residual Cerium Content
of the Steel for Each Heat Modeled at 1700°C

Free energy minimization predicts that cerium will be most effectively removed from the steel by the slags used in heats 77, 80, and 91 and least effectively by the slags used in heats 75, 83, and 86. This is also true for lanthanum. While each slag is predicted to encourage the formation of $AlCeO_3$, the slags used in heats 77, 80, and 91 also permit the formation of CeF_3 and the slag used in heat 77 allows a significant amount of CeO_2 to form as well.

Predictions for Uranium Removal

In order to determine the effect of slag chemistry on predicted uranium partitioning, modeling was performed for stainless steels containing 2500 ppm uranium melted in contact with the same slags used for surrogate modeling at 1700°C. A comparison of the predicted residual uranium content of the steels on a heat by heat basis is presented in Figure 5.

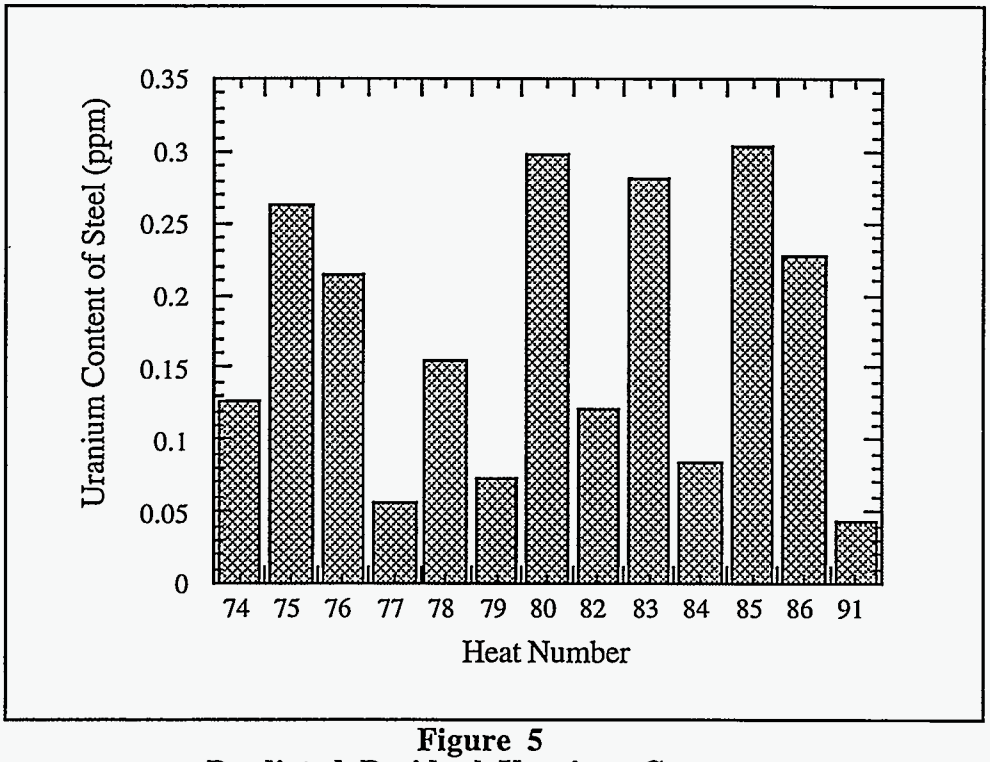

Figure 5
Predicted Residual Uranium Content
of the Steel for Each Heat Modeled at 1700°C

This graph shows that uranium is predicted to be most effectively removed from steel by the slags used for heats 91, 77, 79, and 84 and least effectively removed by the slags used for heats 85, 80, 83, and 75. This suggests that cerium and lanthanum may be collected into the slag by different mechanisms than uranium. Unlike cerium and lanthanum, uranium is not predicted to form aluminates. Free energy minimization does predict the formation of UF_4, but only in minuscule quantities (approximately 1 ppb in the slag). Other uranium species are not predicted, either because thermodynamic data was unavailable or because the presence of

gaseous species such as UF_6 was not predicted when systems were modeled at one atmosphere of pressure. Hence, actual decontamination efficiencies could well be higher than those indicated by Figure 5.

In the modeling performed, the major mechanism by which uranium is removed from the steel is by the formation of UO_2. The slags which should most effectively achieve this removal are those which are able to supply the greatest amounts of available oxygen. When present in a one to one stiochiometric ratio, alumina and calcia are bound together as $CaAl_2O_4$ ($CaO\text{-}Al_2O_3$). Due to the stability of this compound, the oxygen it contains is not available for the oxidation of uranium. If, after the formation of oxygen bearing species more stable than UO_2, excess Al_2O_3 is present, the oxidation of uranium may take place as the free energy of formation of UO_2 per mole of oxygen is more negative than that of alumina at 1700°C.

Differences between Surrogate Elements and Radionuclides

Modeling studies showed that the mechanisms by which uranium is removed from a steel may be different than those by which cerium and lanthanum are removed. Other differences between surrogates and actual radionuclides should be kept in mind when reviewing the results of research performed using surrogates. The physical properties of the compounds which are formed by the radionuclides and surrogates during melt refining affect the partitioning of these elements between the molten metal and the slag. In ESR, elements in the metal may react with free ions in the slag, forming nonmetallic particles. While the densities of the compounds formed by the surrogates are less than that of liquid iron, the densities of the radioactive compounds tend to be much greater. This difference could affect the mechanics of melt partitioning and thus its efficiency.

Slag Skin Thickness and Surface Quality

Although each slag tested in this study was shown to remove the surrogate elements from the bulk of the stainless steel to below detectable levels, the slags were shown to behave differently in other respects. The chemistry of the slag was observed to influence the thickness and texture of the slag skin formed between the water cooled copper crucible wall and the solidified ingot as well as the surface quality of the ingot produced. The average thickness of the slag skin formed during each heat is shown in Figure 6.

The goal of melt decontamination is to concentrate the radioactive elements in a mineral-like solid slag which may be easily packaged for storage. The slag cap resulting from an ESR process tends to be dense and monolithic and, when it fractures, tends to break into large pieces. The slag skin, on the other hand, fractures into many small pieces which, in the process of removing the ingot from the furnace, can generate a great deal of dust. It would be beneficial, therefore, to produce as small a volume of slag skin as possible.

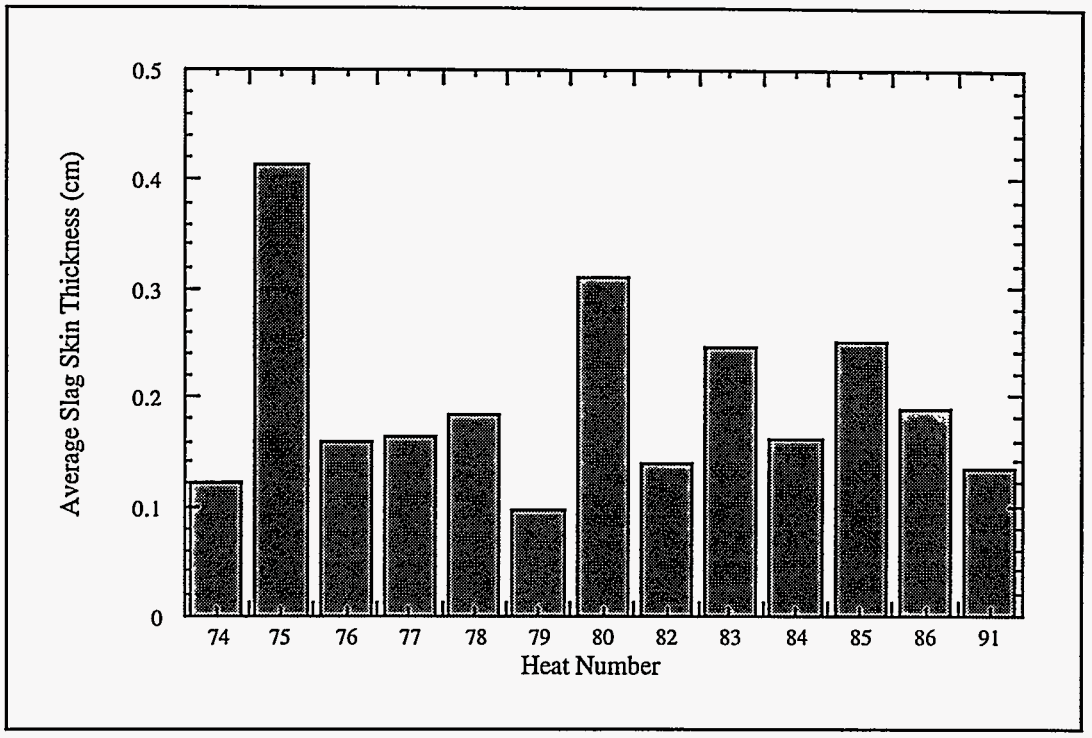

Figure 6
Average Slag Skin Thickness for Each Heat

It was also observed that some ingots had very smooth surfaces while others had rougher surfaces and two ingots, from heats 75 and 85, had slag entrained on their surfaces. Figure 7 shows two ingots, one with an excellent surface and one with a very poor surface.

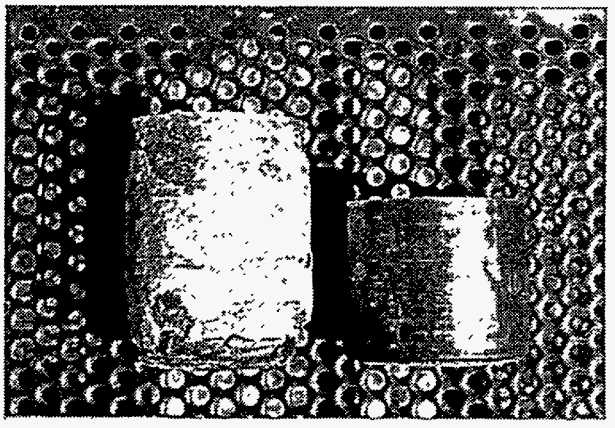

Figure 7
Ingot Sections From Heat 75 (left) and Heat 91 (right)

The surface treatment of ingots produced by the ESR process is expensive and the surface grinding of contaminated ingots could cause additional problems related to the production of radioactive dust. The optimum slag would enable the production of ingots with smooth surfaces, thus reducing the need for surface treatment prior to forming.

A slag skin is formed by the selective solidification of one or more phases on the water cooled copper wall. The phases which solidify and their order of solidification are determined by the composition of the liquid slag and the governing phase relationships as shown by the phase diagram. The constitution diagram of the ternary calcium fluoride-lime-alumina system has been extensively investigated and the diagram shown in Figure 8, prepared by Zhmodin[11], is considered to be the most reliable version. The main feature is a trough corresponding to compositions with roughly equal proportions of lime and alumina. These slags have liquidus temperatures in the range 1350-1500°C which makes them suitable for melting a range of steels and superalloys. Another important feature of the system is a two liquid zone in the high fluoride, low lime region.

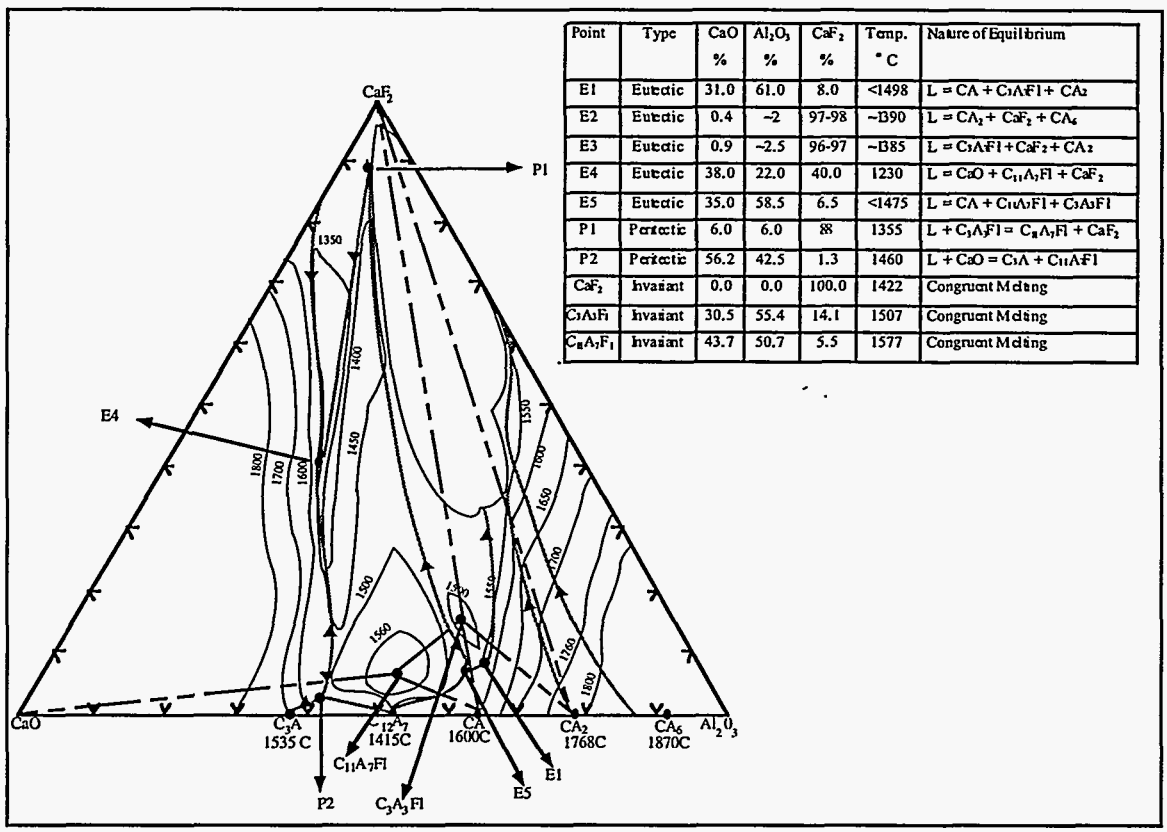

Point	Type	CaO %	Al_2O_3 %	CaF_2 %	Temp. °C	Nature of Equilibrium
E1	Eutectic	31.0	61.0	8.0	<1498	$L = CA + C_3A_3Fl + CA_2$
E2	Eutectic	0.4	~2	97-98	~1390	$L = CA_2 + CaF_2 + CA_6$
E3	Eutectic	0.9	~2.5	96-97	~1385	$L = C_3A_3Fl + CaF_2 + CA_2$
E4	Eutectic	38.0	22.0	40.0	1230	$L = CaO + C_{11}A_7Fl + CaF_2$
E5	Eutectic	35.0	58.5	6.5	<1475	$L = CA + C_{11}A_7Fl + C_3A_3Fl$
P1	Peritectic	6.0	6.0	88	1355	$L + C_3A_3Fl = C_{12}A_7Fl + CaF_2$
P2	Peritectic	56.2	42.5	1.3	1460	$L + CaO = C_3A + C_{11}A_7Fl$
CaF_2	Invariant	0.0	0.0	100.0	1422	Congruent Melting
C_3A_3Fl	Invariant	30.5	55.4	14.1	1507	Congruent Melting
$C_{12}A_7F_1$	Invariant	43.7	50.7	5.5	1577	Congruent Melting

Figure 8
Ternary Phase Diagram for the System CaF_2-CaO-Al_2O_3

Mitchell[12,13,14] has pointed out that the phases present in the slag skin have a direct influence on ingot surface quality. In Figure 9, a solidus diagram for this system[15] has been superimposed over a ternary grid on which the chemistry of each slag used in this study has been plotted.

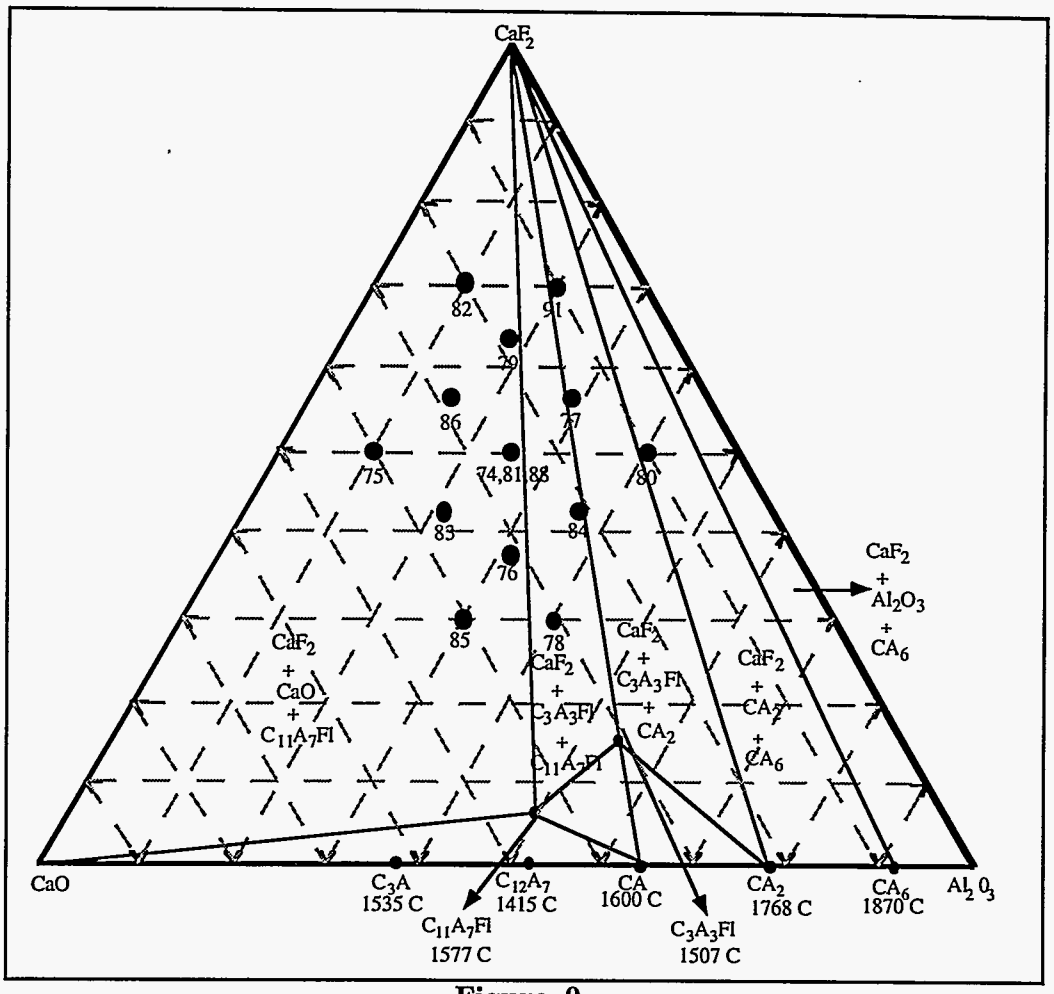

Figure 9
Primary Crystallization Fields for the System CaF_2-Ca0-Al_2O_3 Showing the Phases Which Should Form on Solidification of the Various Slags Tested

For each of the slags used in this study, a solidification path may be traced. The phases which solidify and the order of solidification seem to affect slag skin thickness and ingot surface quality. The slag used in heat 75, for example, produced an ingot with very poor surface quality and yielded the thickest slag skin of any slag studied. The first constituent to solidify was CaO, causing the slag composition to follow a path directly away from the CaO corner of the phase diagram until it intersected a eutectic trough. The composition of the slag followed this trough until the final liquid solidified eutectically at point E4. The slag used in heat 83 was very near the eutectic point E4. The slag used in heat 83 formed a much thinner slag skin and produced a smoother ingot than that used in heat 75, as the solidification path was much simpler. The slag used in heat 79, which yielded the thinnest skin of any slag tested (as well as a very smooth ingot), lies directly on a solidification path terminating with peritectic solidification at point P1. The composition of the slag used in heat 78 lies along the same solidification path as that used in heat 79, although farther from point P1. The longer solidification path followed by slag 78 resulted in a thicker slag skin and a slightly poorer ingot surface than that observed for heat 79.

Of all the slags tested, the two which produced ingots with the smoothest surface were those used in heats 77 and 91. The vertical section of the phase diagram which contains the compositions of both these slags is shown in Figure 10. Solidification proceeds by the formation of a solid and a high fluoride liquid. This solidification path seems to have a beneficial effect on ingot surface quality. This may be due to the presence of a liquid phase during primary solidification or to interfacial tension effects, or both.

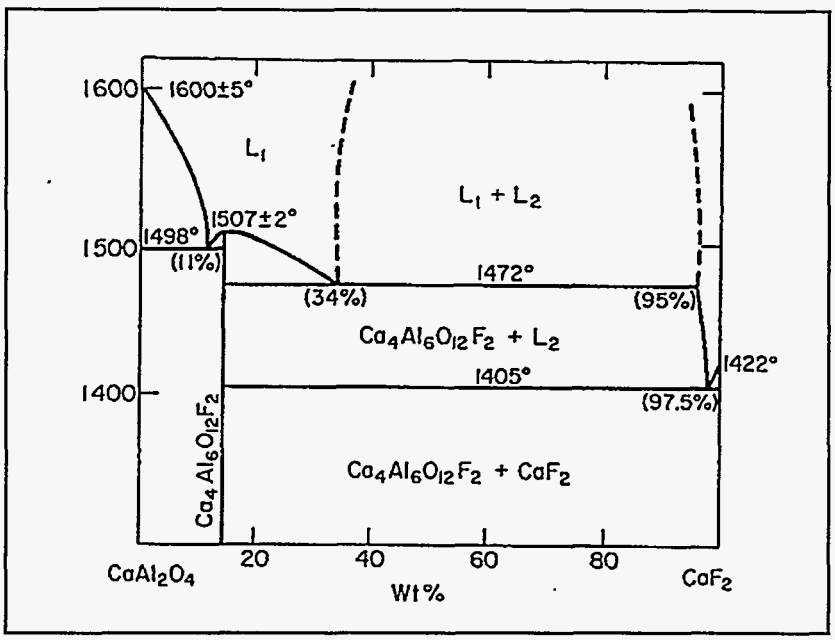

Figure 10
Vertical Section of the Ternary Phase Diagram for the System CaF_2-Ca0-Al_2O_3

CONCLUSIONS AND RECOMMENDATIONS

Slag chemistry was shown to have an impact on the surface quality of the remelted steel and thus on the level of residual surface contamination after melting. The surface quality of the ingots produced by an industrial ESR melt decontamination process would influence the efficiency of this process. Poor surface quality could result in the entrapment of radioactive slag on the ingot surfaces. This contamination would necessitate surface treatment of the ingots before rolling to final shape, resulting in added processing expense, material loss, and exposure of personnel.

Thermodynamic modeling predicted that some slags would allow a higher residual concentration of the surrogate elements in the steel than others. The predicted levels, however, were so low that this could not be confirmed by the results of the melting experiments. Small differences in the level of decontamination achieved could be important, however, especially for highly hazardous elements such as plutonium.

An optimum slag for the melt decontamination of stainless steel would have several attributes. The slag should maximize the extent of decontamination achieved while retaining the chemical pedigree of the alloy. In addition, the slag should solidify in such a manner that a uniformly thin slag skin is produced. This enables the production of ingots with smooth surfaces and uniform grain structure. Of the slags tested, those predicted by free energy minimization to most effectively remove lanthanum, cerium, and uranium from stainless steels were those used in heats 77, 79, and 91. The slag used in heat 79 solidified peritectically to produce the thinnest slag skin of any slag tested. This study indicates that the slag composition used in heat 79, 63.4/18.3/18.3, could be close to optimum for a decontamination slag. Other suitable compositions are expected to lie along the same solidification path. The slag used in heat 79 contains a high percentage of calcium fluoride and is moderately efficient in terms of power consumption. This slag is close in chemistry to 60/20/20, a slag commonly used in industry.

However, thermodynamic modeling suggests that, while the transuranic elements are thermochemically similar to the rare earth surrogates used in this study, they will probably not behave in an identical manner during electroslag remelting operations. It is thus recommended that pilot studies be carried out using actual radioactive elements and that an optimum slag be selected for each type or mixture of contaminants present in each batch of scrap to be melted.

ACKNOWLEDGMENTS

The authors gratefully acknowledge Eric Schlienger and David Melgaard, without whose inspired work on ESR control systems this work would not have been possible.

This work was supported by the United States Department of Energy under Contract DE-AC04-94AL85000. Sandia is a multiprogram laboratory operated by Sandia Corporation, a Lockheed Martin Company, for the United States Department of Energy.

REFERENCES

[1] Dyer, N. C., Bechtold, T.E. (Editor), "Radionuclides in United States Commercial Nuclear Power Reactors," WINCO-1191, INEL-DOE, (1994).

[2] Schwerdtfeger, K, "Some aspects on the kinetics of reactions occurring in the ESRprocess", Proceedings of the 5th International Conference of Vacuum Metallurgy and ESR, Munich Germany (Oct., 1976), 1393-1399.

[3] Duckworth, W.E. and Hoyle, G. Electro-slag Refining, Chapman and Hall Ltd. London, (1969).

[4] Salt, D.J. Electroslag Refining, London, Chapman and Hall. (1969).

[5] Heshmatpour, B., Copeland G.L., Heestand, R.L., "Decontamination of Transuranic Contaminated Metals by Melt Refining," *Nuclear and Chemical Waste Management*, Vol. 4, (1983), 129-134.

[6] F*A*C*T* is a copyrighted product of Thermfact Ltd./Ltee., 447 Berwick Ave., Mount-Royal, Quebec, CANADA, H3r IZ8.

[7] Pelton, A.D., Bale, C.W., "A Modified Interaction Parameter Formalism for Non-Dilute Solutions", *Met. Trans.*, 17A, (1986), 1211-1215.

[8] Kay, D.A.R., Wilson, W.G., Jalan, V. "High Temperature Thermodynamics and Applications of Rare Earth Compounds Containing Oxygen and Sulphur in Fuel Gas Desulphurization and SOx and NOx removal" *Journal of Alloys and Compounds*, Vol. 192, (1993), 11-16.

[9] Kay, D.A.R. "High Temperature Thermodynamics and Applications of Rare Earth Oxides and Sulphides in Ferrous Metallurgy" *Mineral Processing and Extractive Metallurgy Review*, Volume 10, (1992), 307-323.

[10] Eastman, E.D., Brewer, L., Bromley, L. Gilles, P., Lofgren, N. "Preparation and Properties of the Oxide Sulfides of Cerium, Zirconium, Thorium, and Uranium" *Journal of the Americal Chemical Society*, Vol. 73, (1951), 3896.

[11] Chatterjee, A.K., Zhmodin, G.I. "The Phase Equilibrium Diagram of the System CaO-Al2O3-CaF2" *Journal of Materials Science*, Vol. 7, (1972), 93-97.

[12] Mitchell, A. "The Chemistry of ESR Slags" *Canadian Metallurgical Quarterly,* Vol. 20, No. 1, (1981),101-112.

[13] Mitchell, A., Etienne, M. "The Solidification of Electroslag Fluxes" *Transactions of The Metallurgical Society of AIME*, Vol. 242, (July, 1968), 1462-1464.

[14] Bell, M., Mitchell, A., "Some Observations on the Surface Quality of Electroslag Ingots"*Journal of the Iron and Steel Institute*, Vol. 209, Part 8, (Aug., 1971), 658-670.

[15] Mills, K.C., Keene, B.J. "Physicochemical Properties of Molten CaF_2 based slags" *International Metals Reviews*, No 1, (1981), 21-69.

DISCLAIMER

This report was prepared as an account of work sponsored by an agency of the United States Government. Neither the United States Government nor any agency thereof, nor any of their employees, makes any warranty, express or implied, or assumes any legal liability or responsibility for the accuracy, completeness, or usefulness of any information, apparatus, product, or process disclosed, or represents that its use would not infringe privately owned rights. Reference herein to any specific commercial product, process, or service by trade name, trademark, manufacturer, or otherwise does not necessarily constitute or imply its endorsement, recommendation, or favoring by the United States Government or any agency thereof. The views and opinions of authors expressed herein do not necessarily state or reflect those of the United States Government or any agency thereof.